Chiron: Concurrent High Throughput Communication for IoT Devices

Yan Li*
liy1@umbc.edu
Computer Science and Electrical Engineering
University of Maryland, Baltimore County
Johns Hopkins Applied Physics Laboratory

Zicheng Chi*
zicheng1@umbc.edu
Computer Science and Electrical Engineering
University of Maryland, Baltimore County

Xin Liu
xinliu1@umbc.edu
Computer Science and Electrical Engineering
University of Maryland, Baltimore County

Ting Zhu
zt@umbc.edu
Computer Science and Electrical Engineering
University of Maryland, Baltimore County

ABSTRACT

The exponentially increasing number of heterogeneous Internet of Things (IoT) devices motivate us to explore more efficient and higher throughput communication, especially at the bottleneck (i.e., edge) of the IoT networks. Our work, named Chiron, opens a promising direction for Physical (PHY) layer concurrent high throughput communication to heterogeneous IoT devices (e.g., wider-band WiFi and narrower-band ZigBee). Specifically, at the PHY layer, Chiron enables concurrently transmitting (or receiving) 1 stream of WiFi data and up to 4 streams of ZigBee data to (or from) commodity WiFi and ZigBee devices as if there is no interference between these simultaneous connections. We extensively evaluate our system under different real-world settings. Results show that Chiron's concurrent WiFi and ZigBee communication can achieve similar throughput as the sole WiFi or ZigBee communication. Chiron's spectrum utilization is more than 16 times better than the traditional gateway.

CCS CONCEPTS

• **Networks → Network protocol design**; **Home networks**;

KEYWORDS

Wireless, Concurrent Communication, Internet of things (IoT)

1 INTRODUCTION

Internet-of-Thing (IoT) devices use different radios and modulation mechanisms (e.g., WiFi, ZigBee, and Bluetooth). Therefore, they cannot directly communicate with each other. Traditionally, communication between different wireless technologies is achieved indirectly via gateways equipped with multiple radio interfaces.

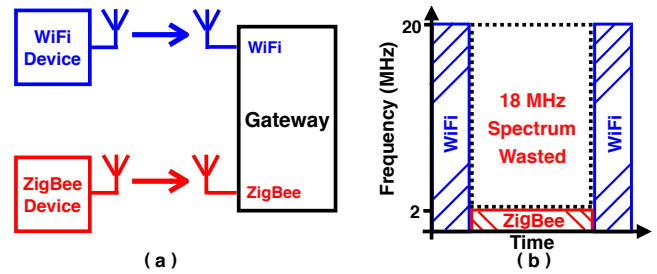*Both authors contributed equally to the paper

Figure 1: Traditional gateway approach has low spectrum utilization, which results in low aggregated throughput.
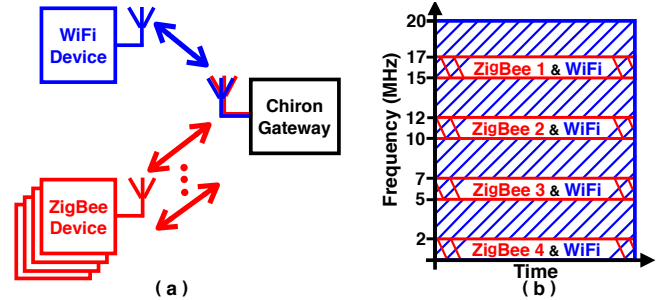

Figure 2: Our approach enables concurrent communications i) from commodity WiFi and ZigBee devices to the gateway; and ii) from the gateway to commodity WiFi and ZigBee devices. Therefore, the spectrum utilization is significantly increased.

The gateway will become a bottleneck when the exponentially increasing number of heterogeneous IoT devices are deployed. For example, in Figure 1, when the WiFi device is transmitting packets to the gateway, the ZigBee device has to back-off to avoid the collision. Similarly, when the ZigBee device is transmitting to the gateway, the WiFi device needs to back-off. Since WiFi's bandwidth (20 MHz) is much higher than ZigBee's bandwidth (2 MHz), when ZigBee is transmitting, WiFi's 18 MHz spectrum that is not overlapped with ZigBee is wasted (shown in Figure 1).

Moreover, we argue that even ZigBee's 2 MHz spectrum may not be fully utilized, because ZigBee's maximum throughput is only

250 kbps, which results in 0.125 bit/s/Hz spectrum utilization. On the other hand, WiFi's spectrum utilization is much higher. For example, with 20 MHz bandwidth, 802.11n can achieve up to 288.8 Mbps throughput [1], which results in 14.4 bit/s/Hz. Therefore, we argue that we should explore a more spectrum efficient and higher throughput communication technique in ZigBee and WiFi coexisted environment.

In this paper, we introduce a new direction for PHY layer concurrent high throughput communication from (or to) heterogeneous (i.e., wider-band WiFi and narrower-band ZigBee) IoT devices. As shown in Figure 2, our work (named Chiron) enables concurrently transmitting (or receiving) 1 stream of WiFi data and up to 4 streams of ZigBee data to (or from) commodity WiFi and ZigBee devices as if there is no interference between these concurrent transmissions. In a nut-shell, Chiron enables the concurrent high throughput communications at the PHY layer by leveraging WiFi and ZigBee signals' unique difference – WiFi's low symbol rate (i.e., 250 Ksymbol/s) verses ZigBee's high chip rate (i.e., 2 Mchip/s). By doing this, we significantly increase the spectrum utilization and overall aggregated throughput among IoT devices.

The main contributions of our work are as follows:

• To the best of our knowledge, this is the first work that enables concurrent high throughput communication i) from the gateway to heterogeneous commodity IoT devices; and ii) from IoT devices to the gateway. Our new gateway design naturally fits at the edge of the IoT networks and can significantly increase the spectrum utilization and overall aggregated throughput.

• To enable the concurrent communication, we addressed several unique challenges, which include i) how to detect and separate the concurrently received WiFi (e.g., IEEE 802.11 g/n) and ZigBee (e.g., IEEE 802.15.4) signals at the gateway; and ii) how to concurrently send out the combined WiFi and ZigBee signals, which can be demodulated by both commodity WiFi devices and commodity ZigBee devices.

• We implemented Chiron on i) commodity WiFi devices; ii) commodity ZigBee devices; and iii) USRP devices. Then, we extensively evaluated our system under four real-world scenarios (i.e., line-of-sight, none-line-of-sight, human in the middle, and wearable). Results demonstrate that Chiron's spectrum utilization is more than 16 times more than the traditional gateway.

2 OBSERVATION AND MOTIVATION

The design of Chiron is motivated by the following observation:
Observation: *Although WiFi and ZigBee communicate at the overlapped radio frequency, WiFi's symbol rate and ZigBee's chip rate [1] are significant different that WiFi's symbol rate is 250 Ksymbols/s while ZigBee's chip rate is 2 Mchips/s.*

This observation serves as the foundation of our design. Figure 3 shows the combined WiFi and ZigBee signal (the black line) in time domain. The red line is the original WiFi signal. From Figure 3, one can tell that WiFi signal's amplitude changes much slower than ZigBee signal's amplitude. Therefore, it is possible to design a

---

[1]ZigBee protocol uses Direct Sequence Spread Spectrum (DSSS) technique, in which, a chip is the smallest unit of a rectangular pulse. Similar to WiFi's symbol rate, ZigBee's chip rate reveals the signal varying speed.
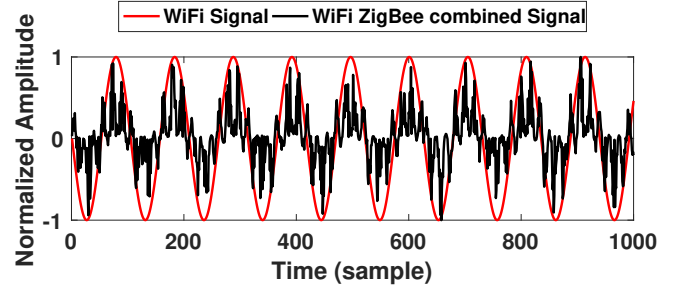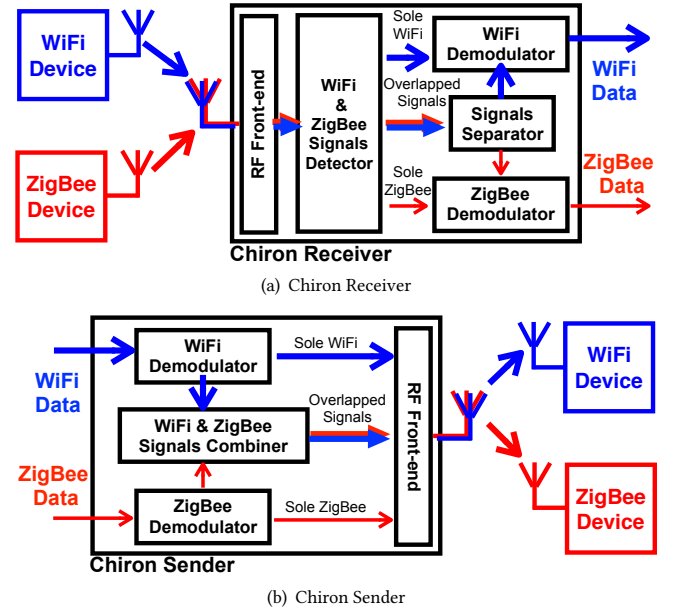

Figure 3: Combined WiFi and ZigBee Signals

(a) Chiron Receiver

(b) Chiron Sender

Figure 4: System Architecture

gateway that can send (or receive) the combined WiFi and ZigBee signal which contains both WiFi data and ZigBee data to (or from) commodity WiFi and ZigBee devices. By doing this, the spectrum utilization and throughput can be significantly increased.

3 DESIGN OVERVIEW AND CHALLENGES

Based on our observation, the design goal of Chiron is to maximize the spectrum utilization when the gateway receives (or transmits) data from (to) commodity WiFi and ZigBee devices. Figure 4 shows Chiron's system architecture. For clarity purpose, we divide the whole system into two parts: i) Chiron Receiver and ii) Chiron Sender.

• **Chiron Receiver (Figure 4(a)):** There are two main challenges in Chiron receiver's design. The *first* challenge is how to incorporate different traffic patterns of wireless traffic generated by commodity WiFi and ZigBee devices at the gateway. To address this challenge, we design a customized WiFi & ZigBee signals detector, which can detect whether

the received signal is a sole WiFi, sole ZigBee or a WiFi and ZigBee overlapped signal. The output goes to i) a WiFi demodulator when sole WiFi signals are detected; ii) a ZigBee demodulator when sole ZigBee signals are detected; or iii) a signal separator when the WiFi and ZigBee overlapped signal are detected. The **second** challenge is how to separate the overlapped signal. To address this challenge, we developed a signal separator by leveraging our observation that the WiFi's symbol rate and ZigBee's chip rate are significantly different. The detailed design is described in Section 5.1.2.

- **Chiron Sender (Figure 4(b)):** The main challenge in Chiron sender's design is how to combine the ZigBee signal with WiFi signal so that the combined signal can be demodulated at both the commodity ZigBee and WiFi receivers' side. To address this challenge, we developed WiFi & ZigBee Signals combiner with a linear optimization algorithm that generates the combined signals and ensures the signal distortion is within the tolerance range of commodity WiFi and ZigBee devices' modulation schemes. The detailed design is described in Section 5.2.

4 BACKGROUND

To explain Chiron, it is necessary to first understand how WiFi and ZigBee radios work. Although our description is specific, our design has the potential to be applied to other heterogeneous radios that share the same frequency band.

4.1 How WiFi transmitter & receiver work

WiFi Transmitter: Figure 5(a) illustrates how the WiFi device transmits information in following steps:

Step 1: The WiFi data goes into a serial to parallel converter which allocates the bits on different subcarriers.

Step 2: On each subcarrier, WiFi modulates information using Quadrature Amplitude Modulation (QAM) by mapping bits to different phases in sine waves.

Step 3: To combine the sine waves efficiently, WiFi adopts orthogonal frequency-division multiplexing (OFDM) by utilizing an inverse fast Fourier transform (IFFT), expressed in Equation 1. The duty cycle that the IFFT operates defines the symbol duration.

$$C_m(t) = \sum_{n=0}^{N} \left[(I(t)\cos(2\pi f t_1) - Q(t)\sin(2\pi f t_1)) e^{2\pi jkn} \right] \quad (1)$$

Where there are N total WiFi subcarriers, and for each n subcarrier, we defined complex symbols states at the $I(t)$ and $Q(t)$ mapped by QAM. The duty cycle of each symbol is defined by f. We defined the subcarrier spacing frequency by k. Thus, $C_m(t)$ is the combined sine waves for mth bits.

Step 4: Between each symbol duration, A cyclic prefix is appended to reduce intersymbol interference. The added cyclic prefix signal is defined as the baseband WiFi signal.

Step 5: Before the baseband WiFi signal, a training sequence allowing for sender and receiver discovery and synchronization is

added. Thus, in a conventional WiFi sender, the baseband and training sequence signals are then up-converter to the desired transmit frequency, amplified, filtered, and radiated by the RF front-end.

WiFi Receiver: Figure 5(b) shows how a WiFi receiver works in following steps:

Step 1: The radio down-converts the WiFi signal to baseband frequencies.

Step 2: The radio attempts to correlate for the training sequence. If the training sequence correlation exceeds the detection threshold, the signal goes to next step.

Step 3: The WiFi receiver will apply a standard FFT to the signal to separate the subcarriers.

Step 4: Multiple QAM subcarriers demodulators map the sine waves' phase states to each symbol state and bit combination.

Step 5: The demodulated bits on each subcarrier are combined by a parallel to serial convertor.

4.2 How ZigBee transmitter & receiver work

ZigBee Transmitter: Figure 6(a) illustrates how a ZigBee transmitter works in two steps:

Step 1: To compensate for channel interference and reduce the transmission power, ZigBee uses Direct Sequence Spread Spectrum (DSSS) to spread the signal into a wider band by multiplying with a higher rate (2 MHz) pseudorandom noise (PN) code. This PN code is shared between the sender and receiver.

Step 2: After the spread spectrum process, the ZigBee modulator maps the bits to sine waves by Offset quadrature phase-shift keying (OQPSK) modulation which reduces the dramatic phase shifts by offsetting the odd and even bits by a distinct period of time. The output of the OQPSK signal is the ZigBee baseband signal described in Equation 2. The output of the modulators is transmitted in the same manner as the WiFi.

$$Z(t) = \sqrt{\frac{2E}{T}} \cos\left(2\pi f t + (2n-1)\frac{\pi}{4}\right), n = 1, 2, 3, 4 \quad (2)$$

Where E is energy per symbol, and T is the symbol duration. The symbol frequency is defined as f with 4 states defined by n.

ZigBee Receiver: Figure 6(b) shows how a ZigBee receiver works described in three steps:

Step 1: The radio down-converts the signal to the ZigBee baseband.

Step 2: The baseband signal is multiplied by or correlated to a shared PN code.

Step 3: If the PN code correlation exceeds the detection threshold, an O-QPSK demodulator maps the sine waves' phase states to each symbol and bit combination.

5 DESIGN OF CHIRON

In this section, we describe the design of Chiron, which includes the receiver and sender parts.

5.1 Receiver

The objective of Chiron receiver is to disentangle the overlapped WiFi and ZigBee signals. However, before this disentanglement happens, the receiver must determine if and when the overlapped
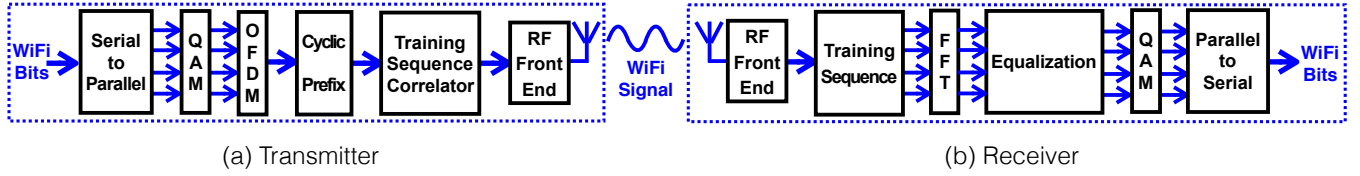
(a) Transmitter

(b) Receiver

Figure 5: The WiFi Transmitter and Receiver

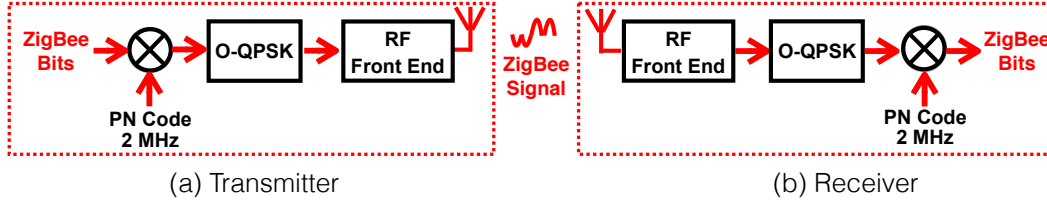
(a) Transmitter

(b) Receiver
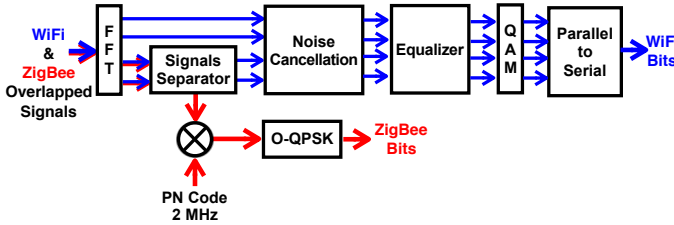
Figure 6: The ZigBee Transmitter and Receiver

Figure 7: The Demodulation of Overlapped WiFi & ZigBee Signals

signal presents. To determine if and when this signal presents, we utilize i) WiFi training sequence and ZigBee PN code correlation; and ii) WiFi Channel State Information (CSI). When the overlapped signal is detected, we use noise cancellation and the native WiFi and ZigBee interference correction mechanism to recover the transmitted data. The following sections detail the i) WiFi & ZigBee signals detection and ii) overlapped WiFi and ZigBee signal receiving.

5.1.1 WiFi & ZigBee Signals Detection. To ensure Chiron works with COTS WiFi and ZigBee devices, Chiron has to be backward compatible with normal WiFi and ZigBee signals. Thus, Chiron must be able to demodulate both the sole WiFi (i.e., a WiFi device is communicating with Chiron gateway without concurrent ZigBee transmission) or ZigBee packets (i.e., a ZigBee device is communicating with Chiron gateway without concurrent WiFi transmission). The first step is to determine whether the incoming signal is WiFi signal, ZigBee signal, or WiFi and ZigBee overlapped signal. This is based on WiFi training sequence ($WiFi\_taining\_seq$ and ZigBee PN code ($ZigBee\_PN$) correlation. To do this, we designed Algorithm 1 as follows. Where acq_signal is the incoming signal. W_t and Z_t are the correlation threshold of WiFi training sequence and ZigBee PN code, respectively. First, we calculate the cross-correlation between incoming signal acq_signal and WiFi training sequence $WiFi\_taining\_seq$ (Line 1). Second, we calculate

the cross-correlation between incoming signal acq_signal and Zig-Bee PN code $ZigBee\_PN$ (Line 2). Finally, we compare the results with the two thresholds W_t and Z_t to determine the signal type (Lines 3-9).

Algorithm 1 WiFi & ZigBee Signals Detection

Input: acq_signal, $WiFi\_taining\_seq$, $ZigBee\_PN$, W_t, and Z_t.
Output: $Type\_signal$.

1: $T_w \leftarrow \int_{-\infty}^{+\infty} acq\_signal * WiFi\_taining\_seq$
2: $T_z \leftarrow \int_{-\infty}^{+\infty} acq\_signal * ZigBee\_PN$
3: **if** $T_w > W_t$ & $T_z < Z_t$ **then**
4: $\quad Type\_signal = WiFi$
5: **else if** $T_w < W_t$ & $T_z > Z_t$ **then**
6: $\quad Type\_signal = ZigBee$
7: **else**
8: $\quad Type\_signal = WiFi + ZigBee$
9: **end if**

If the incoming signal is sole WiFi or ZigBee, the signal feeds into normal WiFi or ZigBee demodulator, respectively. If the signal is determined as overlapped signal, Chiron needs to separate then demodulate it.

5.1.2 Overlapped WiFi and ZigBee Signal. After the WiFi and ZigBee overlapped signal is detected, we must separate and demodulate the signal then apply error correcting mechanism to the distorted signals. For a WiFi and ZigBee overlapped signal (as shown in Figure 7), the ZigBee signal overlaps only portion (7 subcarriers) of the wider frequency-band WiFi signal (consisting of at least 64 subcarriers). Therefore, even when ZigBee signal overlaps with WiFi during the initial training sequence, the training sequence correlation will still exceed the detection threshold. After the training sequence detection, the WiFi carriers are separated by the FFT, the overlapped subcarrier will experience distortions. These distortions are sensed by CSI and pilot tones, identifying the affected subcarriers. The identified ZigBee channel are then

down-converted with the WiFi distortions. To recover from the WiFi distortions, we implemented filters that remove the slower WiFi subcarriers signals from the faster-changing ZigBee chips. After the high-pass filters operating at WiFi subcarriers frequencies, the ZigBee signal is demodulated using the normal demodulator (as we mentioned in Section 4.2) which yields the ZigBee symbols and bits.

As an overview to recover the WiFi bits (shown in Figure 7), first, from the received WiFi signal, we subtract out portions of interfering ZigBee signals. Then, we apply an equalization method on the remaining WiFi signals using a channel sensing technique. Finally, after the signals are demodulated into bits, we apply an error correcting code to the bits associated those equalized and denoised WiFi subcarriers that are overlapped with ZigBee channels. To recover the distorted WiFi signal, we designed four steps shown below:

Step 1: ZigBee Signal Removal: Our ZigBee interference removal functions by removing the higher frequency ZigBee Chips (2 MHz) and leaving the slower WiFi symbol (250 KHz). This is done by a bandpass filter that allows the WiFi signals to proceed and suppressing the ZigBee signal. Thus, this filtering process only occurs on the portion of WiFi subcarriers that are overlapped by the ZigBee signal.

Step 2: Environmental Noise cancellation: Chiron must correct phase noise from ZigBee signal filter and environmental noise (such as human, transmitter, and receiver movements). Because of human movements and objects that reflect RF signals, the WiFi channel can experience strong frequency selective fades. Moreover, Chiron's concurrent communication also causes distortions within specific frequency bands. To remove the frequency and phase distortions, we utilize pilot tones that are sine waves agreed upon by the transmitter and receiver. Therefore, pilot tones estimate the channel interference, and then Chiron corrects the interference as follows:

First, the receiver measures the received pilot tone sine wave represented in complex format. Then, the receiver computes the offset between the agreed upon expected sine wave expressed in Equation 3. Finally, by computing the correction factor a and b, the receiver applies a correction to all the subcarriers around pilot tone's frequency.

$$a \cdot I(t) \cos(2\pi f t) - b \cdot Q(t) \sin(2\pi f t) \qquad (3)$$

Where, $I(t)$ and $Q(t)$ represent the complex sine wave of a pilot tone, and a and b represent interference added to the pilot tones and the correction factor.

Step 3: WiFi Demodulation: These equalized quadrature signals are sent to the normal WiFi OFDM demodulation systems and the original WiFi bits are recovered (as we introduced in Section 4.1).

Step 4: Forward Error Correction: After the WiFi bits are demodulated from each WiFi subcarrier, we note that the ZigBee overlapped subcarriers have a higher bit error rate. Moreover, the overlapped ZigBee packets also have a higher probability of error. By appending Forward Error Correcting (FEC) to the data stream
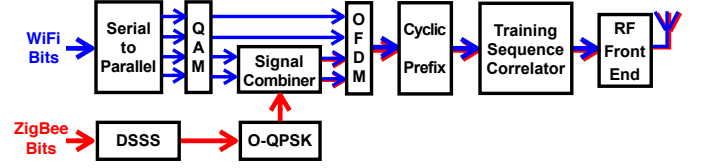

Figure 8: WiFi & ZigBee Signals Combiner

during concurrent communication, we can also increase the probability of correct reception. Because the corruption in the WiFi bitstream can be expected, as ZigBee packets are transmitted within a fixed frequency band, we can append extra FEC to non-affected bits. We utilize a fast linear FEC Low-density parity-check code (LDPC) to be compatible with modern 802.11 standards. By utilizing LDPC's sparse parity matrix, Chiron spread the parity information across the payload frame. To be compatible with commodity devices, we increased the convolutional coding FEC rate. Additionally, interleaving bits during formation of the FEC increases the likelihood of packet reception.

5.2 Sender

Figure 8 shows an overview of the Chiron sender. 1) First, the WiFi signals are parallelized and mapped by QAM, and the ZigBee bits are modulated by DSSS and O-PQSK (detailed in Section 4). 2) The overlapped WiFi subcarriers are combined with ZigBee sine waves. 3) Both the overlapped and the regular WiFi subcarriers are efficiently combined using OFDM. 4) Finally, a cyclic prefix and training sequence is appended to the signal and sent to the RF frontend.

To transmit the signals concurrently, the output of the wider-band WiFi signal must contain similar signals as the output of the ZigBee and desired WiFi. Thus, a portion of the signals from the WiFi QAM modulator will contain distorted signals. The distortion must not exceed the interference tolerance of WiFi's OFDM and ZigBee DSSS modulation schemes. We describe a linear optimization algorithm that combines both WiFi subcarriers to contain both WiFi and ZigBee signals. This combination is possible because the chip rate and the symbol rate of WiFi and ZigBee are significantly different. To combine the ZigBee and WiFi signal, we recognize that 7 WiFi subcarriers overlap a single ZigBee channel. Thus, the overlapping WiFi subcarriers, which operates with 312.5 KHz offsets, must contain both the higher 2 MHz frequency ZigBee chips rate and the lower 250 WiFi KHz symbol rate. To create this combined signal, we use linear programming with weights.

We set up the linear programming model as a maximization model. Chiron adds WiFi subcarrier sample instant with a weighted ZigBee sample instant expressed in Equation 4. The maximizing constraint is the matching of the combined output signal to both the original ZigBee and WiFi signals (Equation 5). To measure how well the combined signals matches, we use cross-correlation. Therefore, the maximizing constraints are cross-correlation between the combined sub-carriers and 1) the original WiFi sub-carriers and 2) the spread signal ZigBee signal.

To achieve this maximizing objective, we solve for optimal weights that are added to WiFi subcarrier, expressed in equations 4 and 5.
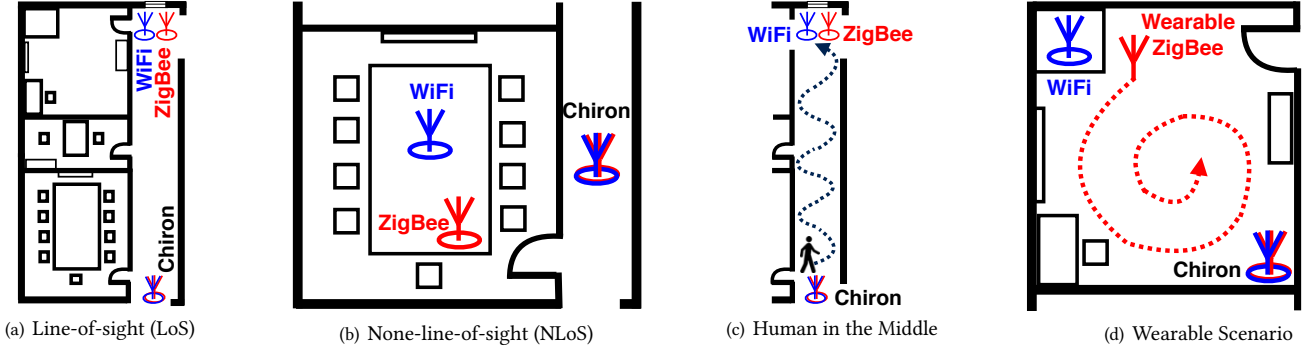
(a) Line-of-sight (LoS)   (b) None-line-of-sight (NLoS)   (c) Human in the Middle   (d) Wearable Scenario

Figure 9: Four Experimental Scenarios

Where n to d index of the overlapping WiFi subcarriers, C_m is the WiFi QAM modulated sine wave, $Z(l)$ is the ZigBee signal, and w is the weight applied per ZigBee sine wave. The subcarriers are efficiently combined using an IFFT, expressed by the equation $e^{e\pi jkt}$. By solving the weights using a linear optimization technique, we efficiently combine the WiFi subcarriers described in without having to resort to multiple subcarriers down and up conversions and filtering. The optimal resulting weights represent the higher frequency distortion factors added to each WiFi subcarrier. Thus, this linear programming results yields an efficiently combined WiFi and ZigBee signal.

$$
\begin{aligned}
Max \\
w \in R
\end{aligned}
\left[
\begin{array}{l}
\sum_{t=0} B^* \left(w(t_1) \right) \cdot C \left(t_1 + n \right), \\
\sum_{t=0} B^* \left(w(t_2) \right) \cdot Z \left(t_2 + n \right)
\end{array}
\right]
\tag{4}
$$

subject to

$$
B(w(t)) = \sum_{n=0}^{N} \left(C_m(t) + w(t) \cdot Z(t) \right) e^{2\pi jkn}
\tag{5}
$$

In the combined WiFi and ZigBee signal, the ZigBee signal is typically longer than the WiFi packet. To solve this problem of different packet length, we leverage nulling out the WiFi signals expressed in Equation 5. C_m is zero, and the ZigBee signal $Z(t)$ with the weight w is left. Therefore, the overlapping subcarriers are left with only the ZigBee signals when the ZigBee signal is longer than the WiFi signal.

6 EXPERIMENTAL EVALUATION

In this section, we introduce our evaluation of Chiron with different metrics (i.e., spectrum utilization, throughput, bit error rate and packet recaption ratio) in four real-world scenarios.

6.1 Experimental Setup

We evaluated our Chiron system in an engineering building, which has a lot of other WiFi access points, Bluetooth devices, and ZigBee devices that create interference. We conducted experiments under four scenarios (shown in Figure 9):

• **Line-of-sight (LoS):** The Chiron gateway and WiFi/ZigBee devices are in Line-of-sight (shown in Figure 9(a)).

• **None-line-of-sight (NLoS):** The Chiron gateway and WiFi/ZigBee devices are placed in different rooms (shown in Figure 9(b)).

• **Human in the Middle:** During human in the middle scenario, a person walks in the trajectory shown in the black dashed line (shown in Figure 9(c)).

• **Wearable Scenario:** In the wearable scenario, a person carries a ZigBee device and walks in the trajectory. As described in the white paper from ZigBee Alliance [3], ZigBee radios are used in wearable applications, such as chronic disease management, health, and wellness (shown in Figure 9(d)).

In the LoS, NLoS and human in the middle scenarios, we vary the communication distance between Chiron gateway and the WiFi/ZigBee devices. Note that the distance between the WiFi and ZigBee is fixed because the gateway-to-WiFi's communication distance does not impact the communication from the gateway to ZigBee, and vice versa.

In our experiment, the design of Chiron gateway (described in Section 5) is implemented on a USRP. We used a commodity DELL XPS 9550 laptop's WiFi card and TelosB [2] as the WiFi and ZigBee devices, respectively, to communicate with Chiron gateway for evaluation. Since Chiron technique focuses on physical layer concurrent communications while the application profile may affect the measured benefit of Chiron, in this evaluation we focused entirely on the physical layer to explore the advantages of Chiron.

For each data point, we transmitted and received around 5 million bits. The following metrics are used to evaluate the Chiron system:

• **Throughput:** successfully received bits divide by the transmission time.

• **Bit Error Rate (BER):** the number of successfully received bits divided by the number of transmitted bits.

• **Packet Reception Ratio (PRR):** the number of successfully received packets divided by the number of transmitted packets.

• **Spectrum Utilization:** throughput per second per hertz at the receiver side.

To compare with Chiron which can conduct concurrent communications between WiFi and ZigBee, we also implemented the following schemes:
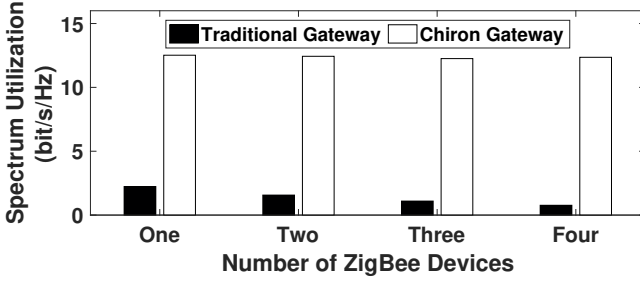
Figure 10: Spectrum Utilization: since Chiron can concurrently communicate to both the WiFi and ZigBee devices, Chiron gateway's spectrum utilization is 16X better than that of the traditional gateway when the number of ZigBee devices is 4.

• **Sole WiFi-to-Gateway or Sole Gateway-to-WiFi:** In these two schemes, a WiFi device is transmitting (or receiving) packets to (or from) our gateway without the concurrent transmission of ZigBee devices. These two schemes serve as the upper bound of the achievable throughput for WiFi communication in real-world settings. We note that there exists the interference from the other IoT devices' wireless traffic inside the building.

• **WiFi-to-Gateway with ZigBee traffic or ZigBee-to-Gateway with WiFi traffic:** These two schemes represent the traditional gateway's performance in real-world scenarios, in which WiFi devices are competing with ZigBee devices for sending the packets to our gateway. This serves as the baseline.

• **Sole ZigBee-to-Gateway or Sole Gateway-to-ZigBee:** In these two schemes, one or multiple ZigBee devices are transmitting/receiving packets to/from the gateway without concurrent WiFi transmission. When we evaluate ZigBee communication, these two schemes serve as the upper bound of the achievable throughput.

• **Gateway-to-ZigBee with WiFi traffic or Gateway-to-WiFi with ZigBee traffic:** These two schemes represent the traditional gateway's performance while sending in real-world scenarios, in which WiFi packets and ZigBee packets are allocated to different time slots to avoid collision. This serves as the baseline.

6.2 Overall Performance

In this section, we evaluate the overall performance, which includes spectrum utilization and throughput of Chiron. In this experiment, we set one COTS WiFi device and multiple COTS ZigBee devices communicating with the gateway. For traditional multi-radio gateway approach, these devices communicate in a TDMA manner, because concurrent communications are not allowed. For Chiron, these devices conduct concurrent communications as stated in Section 5.

6.2.1 Spectrum Utilization. To show the significant benefit of Chiron, we first evaluate the spectrum utilization in heterogenous networks (WiFi and ZigBee devices coexist). Figure 10 shows the comparison between traditional multi-radio gateway and Chiron
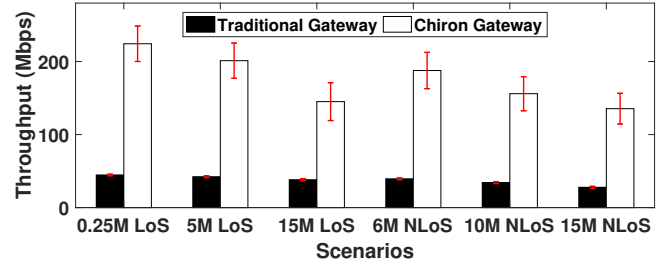

Figure 11: Overall Throughput: across all the communication distances for both the LoS and NLoS scenarios, the throughput of Chiron (up to 224.34 Mbps) is higher than traditional gateway.

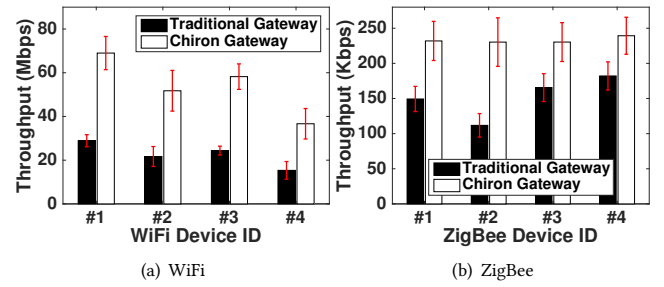

(a) WiFi   (b) ZigBee

Figure 12: Multiple WiFi and ZigBee Devices Communicate with Chiron Gateway: Chiron gateway can concurrently communicate with four different ZigBee devices (which are on different ZigBee channels) while communicating with different WiFi devices alternatively.

gateway. In traditional multi-radio gateway approach, the gateway has to allocate ZigBee and WiFi packets into different time slot, which yields a very low spectrum utilization of 2.34 bit/s/Hz and 0.767 bit/s/Hz when there are one and four ZigBee senders.

For Chiron, since it can concurrently communicate with both the WiFi and ZigBee devices, the spectrum utilization is much higher than traditional multi-radio gateway. When the number of ZigBee is four, the spectrum utilization of Chiron gateway can achieve 12.355 bit/s/Hz which is more than 16X better than traditional Gateway.

6.2.2 Overall Throughput. We show the overall throughput of Chiron comparing with multi-radio gateway. The overall throughput includes both the WiFi and ZigBee parts. As shown in Figure 11, across all the communication distances for both the LoS and NLoS scenarios, Chiron features the higher throughput than the traditional gateway. When the distance is 0.25 meters in LoS, the overall throughput of Chiron is 224.34 Mbps which shows more than 4X higher than of traditional gateway. The reason is Chiron can conduct concurrent WiFi and ZigBee communications (as described in previous sections) while the traditional scheme only allow one type communication (with either WiFi or ZigBee) at a time.

6.2.3 Throughput in Multiple WiFi and ZigBee. This section demonstrates Chiron can communicate with multiple WiFi and

(a) One ZigBee
(b) Four ZigBee
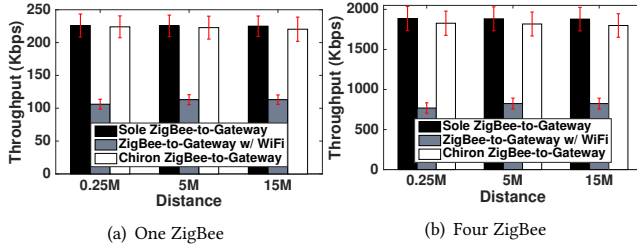
Figure 13: Throughput of ZigBee-to-Gateway Link: When WiFi traffic exists, the throughput of Chiron ZigBee-to-Gateway is about 2.3 times higher than traditional gateway approach. Besides, Chiron ZigBee-to-Gateway is similar to sole ZigBee-to-Gateway which does not have WiFi traffic interference.

ZigBee devices. Figure 12(a) shows the throughput across four different WiFi devices. Since all of the four WiFi devices work on the same frequency band, they share the 20 MHz bandwidth in terms of frequency and transmit (or receive) at different time to avoid collision. The aggregated throughput of Chiron gateway is around 200 Mbps which is similar to the single WiFi communication as shown in Figure 11. Compared with the traditional gateway approach, the aggregated throughput of Chiron is more than two times higher because the communications between WiFi and gateway are not interrupted by the ZigBee communication. Figure 12(b) shows the throughput across four different ZigBee devices. For Chiron gateway, we observed that all of the four ZigBee devices can achieve a high throughput (up to two times better than the traditional gateway approach) because the 20MHz WiFi channel is overlapped with up to four ZigBee channels. Therefore, the Chiron gateway can communicate with four ZigBee devices on four different channels and have negligible impact to the concurrent communication between the Chiron gateway and WiFi devices.

6.3 Receiver Evaluation

In this section, we introduce the performance of Chiron receiver in which both the COTS WiFi and ZigBee devices transmit to the Chiron gateway.

6.3.1 ZigBee-to-Gateway Communication. **Throughput:** To illustrate the effectiveness of Chiron on ZigBee-to-Gateway link, we first compare its throughput with sole ZigBee-to-Gateway (i.e., communications between COTS ZigBee device and COTS multi-radio gateway by using normal ZigBee protocol). The results are shown in Figure 13. In Figure 13(a), one ZigBee device communicates with either one ZigBee gateway (native ZigBee-to-Gateway) or the Chiron gateway (Chiron ZigBee-to-Gateway). We can observe that the throughput of Chiron ZigBee-to-Gateway (the mean value is 223.97 Kbps at 0.25 meter) is very close to sole ZigBee-to-Gateway on different communication distances and approaching the cap of theoretical ZigBee protocol's throughput. Also, the performance is stable on different communication distances (the mean value is 220.32 Kbps at 15 meters). Further, while comparing Chiron ZigBee-to-Gateway with ZigBee-to-Gateway with WiFi traffic

(a) LoS
(b) NLoS
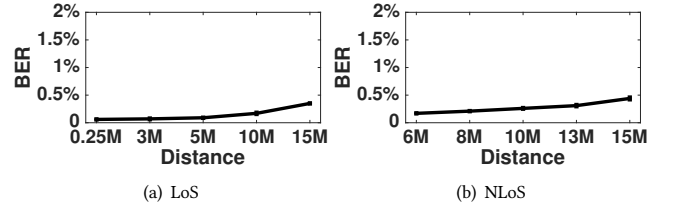
Figure 14: Bit Error Rate of ZigBee-to-Gateway Link: Chiron ZigBee-to-Gateway link's BERs are lower than 0.5% across different distances in both LoS and NLoS scenarios.

(the grey bar), Chiron ZigBee-to-Gateway is about 2.3 times of ZigBee-to-Gateway with WiFi traffic because Chiron gateway can concurrently receive from both the WiFi and ZigBee receivers.

Since one WiFi channel can overlap with up to four ZigBee channels, we evaluated four ZigBee devices communicating with either another four ZigBee devices (sole ZigBee-to-Gateway) or the Chiron gateway (Chiron ZigBee-to-Gateway) and show the aggregated throughput in Figure 13(b). By looking at the results, the performance is still stable across all of the communication distances. The difference between native ZigBee-to-Gateway and Chiron ZigBee-to-Gateway is very small even at 15 meters. However, when WiFi traffic exists, Chiron ZigBee-to-Gateway shows big advantage comparing with native ZigBee-to-Gateway with WiFi.

The reasons Chiron can achieve comparable throughput of Zig-Bee protocol even under WiFi interference are: i) the Chiron gateway can demodulate original OQPSK signal (modulation scheme adopted by ZigBee protocol); and ii) Chiron can demodulate ZigBee signal along with overlapped WiFi signal as introduced in Section 5.
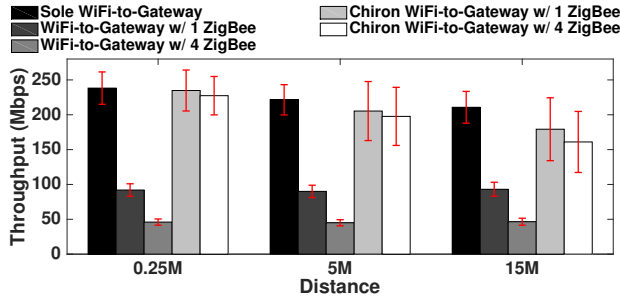
Bit Error Rate: Figure 14 shows the Bit error rate (BER) of Chiron ZigBee-to-Gateway link. Though ZigBee signal is overlapped with WiFi signal at Chiron gateway side, our technique (introduced in Section 5) is still able to differentiate them and demodulate them. Thus, the ZigBee-to-Gateway link BER still follow the characteristic of OQPSK (ZigBee's modulation scheme). Figure 14(a) shows the BER in LoS scenario, we can observe that all of the BERs are lower than 0.5%. In NLoS scenario (Figure 14(b)), all of the BERs are still lower than 0.5% but the average is higher than in LoS scenario. This is because the direct path is blocked and the multipath effect is more complicated in NLoS scenario.

Packet Reception Ratio: The Chiron gateway is able to demodulate ZigBee and WiFi overlapped packet. To confirm the effectiveness, we conducted experiments to evaluate the Packet reception ratio (PRR) in this section. Figure 15 shows the PRR of Chiron ZigBee-to-Gateway link. In LoS scenarios (Figure 15(a)), when the communication distance is short (at 0.25 meter), the PRR can achieve 95%. When the communication distance increases, the PRR drops and reaches 70.4% when the distance is 15 meters. In NLoS scenarios (Figure 15(b)), because of rich multipath effects and propagation loss, the PRR drops a little bit. The value is 84.4% at 6 meters. This experiments validated the ZigBee-to-Gateway communication along with WiFi communication in Chiron.
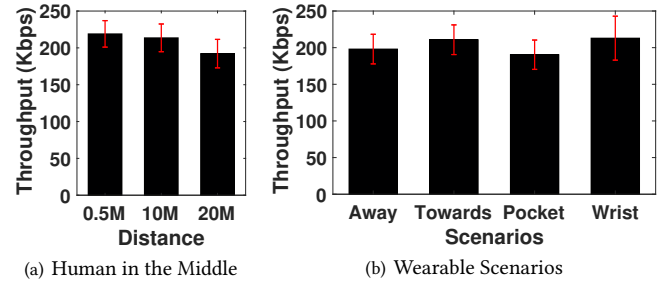
(a) LoS

(b) NLoS
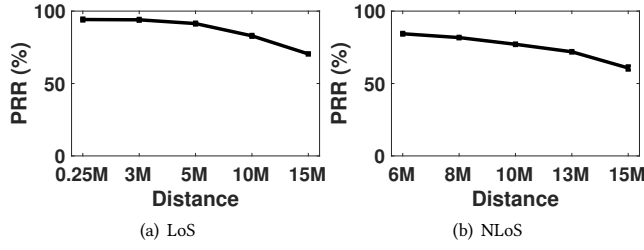
Figure 15: Packet Reception Ratio of ZigBee-to-Gateway Link: Chiron ZigBee-to-Gateway link achieve an up to 95% PRR, even when the distance increases to 15 meters, the PPR can still reach 70.4%.

(a) Human in the Middle

(b) Wearable Scenarios

Figure 17: ZigBee-to-Gateway Throughput in Mobile Scenarios: The performance is stable in different mobile scenarios.

Figure 16: Throughput of WiFi-to-Gateway Link: Chiron shows similar throughput to sole WiFi-to-Gateway but almost 4 times of traditional gateway approach when four ZigBee devices exist.

6.3.2 WiFi-to-Gateway Communication. In this section, we evaluate the WiFi-to-Gateway link of Chiron. To do this, we first compare the performance of sole WiFi-to-Gateway (i.e., a WiFi device communicates with a COTS multi-radio gateway without ZigBee traffic) with Chiron WiFi-to-Gateway (i.e., concurrent transmission with ZigBee-to-Gateway link). We conducted the experiments with either one ZigBee device or four ZigBee devices because one 20 MHz WiFi channel can overlap with up to four ZigBee channels. The results are shown in Figure 16, we observe that the throughput of Chiron WiFi-to-Gateway can achieve similar level of sole WiFi-to-Gateway. When the distance is close (i.e., at 0.25 meter LoS), Chiron WiFi-to-Gateway with one ZigBee and four ZigBee only show 1.4% and 4% difference comparing with native WiFi-to-Gateway, respectively. When the distance is long, the difference increases because at the gateway side, Chiron encounters interference from either one or four ZigBee devices. However, by resolving the interference (as stated in Section 5), the Chiron WiFi-to-Gateway throughput with one ZigBee and four ZigBee are only 7.3% and 15% lower than native WiFi-to-Gateway, respectively, at 15 meters.

Then, we compare the throughput while ZigBee traffic exists. At 0.25 meter, Chiron WiFi-to-Gateway is 1.55X and 3.94X times high the normal WiFi-to-Gateway while one or 4 ZigBee devices are communicating with the gateway, respectively. At 15 meters, we also observe similar increases. The reason is that different normal

multi-radio gateway, Chiron gateway is able to disentangle and demodulate WiFi and ZigBee signals concurrently.

6.3.3 Mobile Scenarios. To extensively evaluate the robustness of Chiron, we conducted an experiments with a designated person walking in the middle of sender and receiver (as shown in Figure 9(c)). Moreover, to evaluate the wearable applications (such as health and wellness monitoring [3]), we also asked the participant wearing the ZigBee device (in pocket or on wrist) and performing daily activities (shown in Figure 9(d)).

ZigBee-to-Gateway: Figure 17(a) shows the ZigBee-to-Gateway link throughput with human walking in the middle. The throughput is relative stable because the native ZigBee modulation scheme is well adopted in Chiron that the OQPSK-DSSS scheme is robust to environment noise. Comparing with direct LoS scenario (Figure 13(a)), the performance only drops 2% when the communication distance is short. When the communication distance increases to 20 meters, the throughput drops 6.4%.

Figure 17(b) shows four wearable scenarios: i) person walks away from the Chiron gateway with ZigBee sender in pocket; ii) person walks towards from the Chiron gateway with ZigBee sender in pocket; iii) person walks around the meeting room with ZigBee sender in pocket; and iv) person walks around the meeting room with ZigBee attached to the wrist. We can observe the fluctuation across the four wearable scenarios. However, overall, the performance is stable. The lowest throughput still can achieve 190 Kbps when the person walks around the meeting room with ZigBee sender in pocket.

WiFi-to-Gateway: Figure 18 shows the WiFi-to-Gateway link throughput. In human in the middle (Figure 18(a)), the WiFi-to-Gateway link maintains up to 226.2 Mbps. However, different from ZigBee-to-Gateway link, the performance drops relatively quickly because the sophisticated modulation scheme (which adopts by WiFi protocol) suffers more degradation in multipath rich environment. In wearable scenario (Figure 18(b)), the red error bar (which indicates the standard deviation) has an average value of 25%, which means the WiFi-to-Gateway links fluctuates due to the advanced modulation scheme defined by WiFi standard.
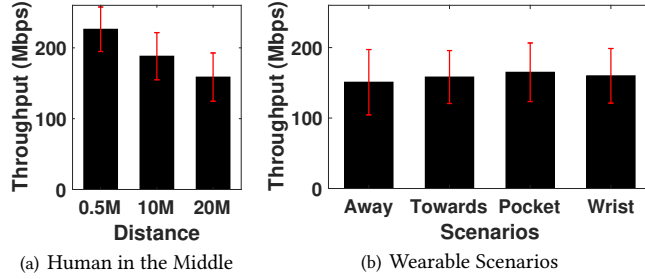
(a) Human in the Middle

(b) Wearable Scenarios

Figure 18: WiFi-to-Gateway Throughput in Mobile Scenarios: Results shows Chiron is robust in different real-world setup.
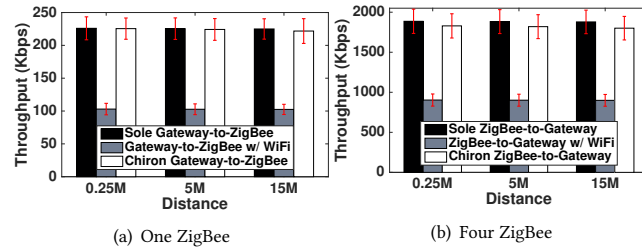

(a) One ZigBee

(b) Four ZigBee

Figure 19: Throughput of Gateway-to-ZigBee Link: When WiFi presents, Chiron is able to double the throughput comparing with the traditional gateway approach because Chiron can concurrently transmit to both the WiFi and up to four ZigBee device.

6.4 Sender Evaluation

In this section, we evaluate the performance of Chiron sender in which the Chiron gateway concurrently transmit to both the COTS WiFi and ZigBee devices. To illustrate the robustness of Chiron, we extensively evaluate it in multiple stationary and mobile scenarios.

6.4.1 Gateway-to-ZigBee Communication. **Throughput:** Figure 19 shows the comparison among sole Gateway-to-ZigBee (i.e., COTS multi-radio gateway communicates with ZigBee device without WiFi traffic), Gateway-to-ZigBee with WiFi traffic (i.e., COTS multi-radio gateway communicates with both ZigBee and WiFi devices), and Chiron Gateway-to-ZigBee (i.e., concurrently sending to both ZigBee and WiFi devices). Figure 19(a) shows the result of the gateway communicating with either one ZigBee device. In which the throughput of Chiron Gateway-to-ZigBee is almost the same with sole Gateway-to-ZigBee on different communication distances and approaching the cap of theoretical ZigBee protocol's throughput (250 Kbps). However, while WiFi messages exist, the multi-radio approach (the bar labeled with Gateway-to-ZigBee w/ WiFi in Figure 19(a)) is half of our Chiron approach because Chiron features concurrent transmissions to both ZigBee and WiFi.

As we mentioned in Section 6.3, one WiFi channel is able to overlap with up to four ZigBee channels. Therefore, we also evaluated four multi-radio gateways (sole Gateway-to-ZigBee) or the Chiron gateway (Chiron Gateway-to-ZigBee) communicating with four
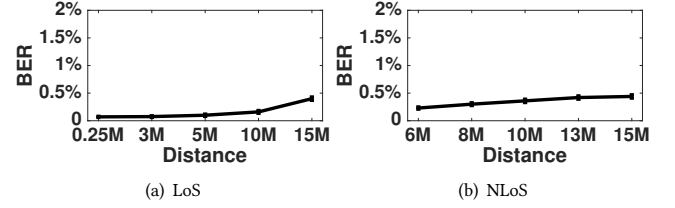

(a) LoS

(b) NLoS

Figure 20: Bit Error Rate of Gateway-to-ZigBee Link: The BER remains low (less than 0.5%) even in NLoS scenario.
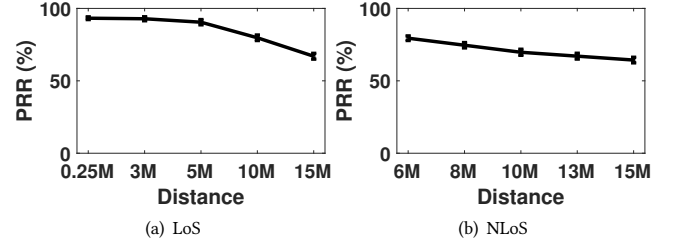

(a) LoS

(b) NLoS

Figure 21: Packet Reception Ratio of Gateway-to-ZigBee Link: When transmitting to both the WiFi and ZigBee devices, the PRR still achieves up to 93.2%.

ZigBee devices. The aggregated throughput is shown in Figure 19(b). By looking at the figure, we can also conclude the throughput of Chiron Gateway-to-ZigBee is two times of the normal multi-radio approach when WiFi traffic exists.

The reason Chiron can double the throughput when communicates with both WiFi and ZigBee devices is that at Chiron gateway, it is able to combine the WiFi and ZigBee signals together, but the signal can be demodulated at COTS WiFi and ZigBee receivers' side.

Bit Error Rate: Figure 20 shows the BER of Gateway-to-ZigBee link in both the LoS. The average BER are all lower than 0.5% at different distance (even at 15 meters) because the DSSS (direct-sequence spread spectrum) is inherited (from ZigBee protocol) in Chiron Gateway-to-ZigBee Link.

Packet Reception Ratio: The Chiron gateway is able to send ZigBee and WiFi combined packet. To confirm the effectiveness, we conducted experiments to evaluate the Packet reception ratio (PRR) in this section. Figure 21 shows the PRR of Chiron Gateway-to-ZigBee link. In LoS scenarios (Figure 21(a)), when the communication distance is short (at 0.25 meter), the PRR is around 93.2%. When the communication distance increases, the PRR drops and reaches 69.7% when the distance is 15 meters. In NLoS scenarios (Figure 21(b)), because of rich multipath effects and propagation loss, the PRR is a little bit lower comparing with in LoS scenario. The value is 79.4% at 6 meters. This experiments validated the Gateway-to-ZigBee communication along with WiFi communication in Chiron.

6.4.2 Gateway-to-WiFi Communication. To show the concurrent sending capacity of Chiron, we compare the performance of sole Gateway-to-WiFi (no ZigBee traffic) and Gateway-to-WiFi with ZigBee traffic with Chiron Gateway-to-WiFi (results are shown in
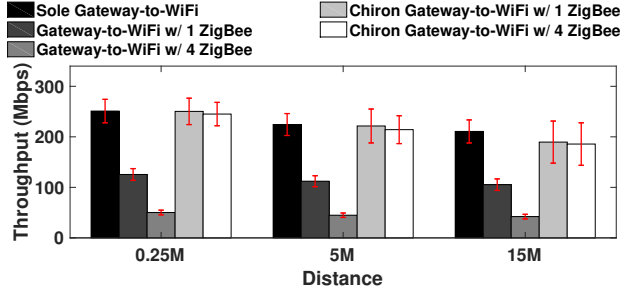
Figure 22: Throughput of Gateway-to-WiFi Link: Chiron shows about 5 times of the traditional gateway approach when transmitting to four ZigBee devices concurrently.

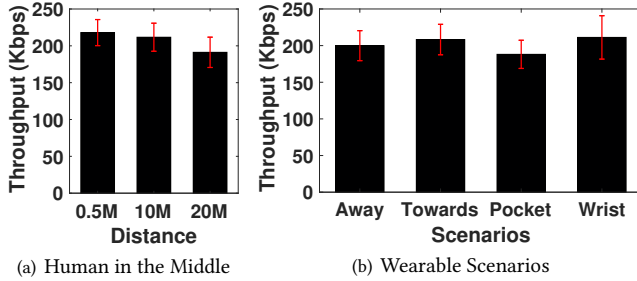(a) Human in the Middle

(b) Wearable Scenarios

Figure 23: Gateway-to-ZigBee Throughput in Mobile Scenarios: The throughput is very close to that in LoS scenario, which validate the robustness of Chiron.

Figure 22). When there is no ZigBee message to send we observe that the throughput of Chiron Gateway-to-WiFi can achieve similar level of sole Gateway-to-WiFi. If the gateway has ZigBee message, our Chiron design shows huge benefit. When the gateway needs to communicate with one ZigBee, Chiron Gateway-to-WiFi shows two times better performance comparing with the normal multi-radio gateway approach. Furthermore, when communicating with four ZigBee devices, Chiron shows almost four times better performance comparing with the normal multi-radio gateway approach. The reason is that Chiron can better utilizes the spectrum to embed ZigBee signal into WiFi signal. Since one 20 MHz WiFi channel is overlapped with up to four ZigBee channels, the Chiron gateway is able to communicate with four ZigBee receivers along with one WiFi receiver.

6.4.3 Mobile Scenarios. To fit Chiron in mobility applications, we also evaluated it in human in the middle (as shown in Figure 9(c)) and wearable scenarios (as shown in Figure 9(d)).

Gateway-to-ZigBee: Figure 23(a) shows the Gateway-to-ZigBee link throughput with human walking in the middle. The throughput is relative stable because the native ZigBee modulation scheme is well adopted in Chiron that the OQPSK-DSSS scheme is robust to environment noise. Comparing with direct LoS scenario (Figure 19(a)), the performance only drops 3% when the communication distance is short. When the communication distance increases to 20 meters, the throughput drops 7.6%.
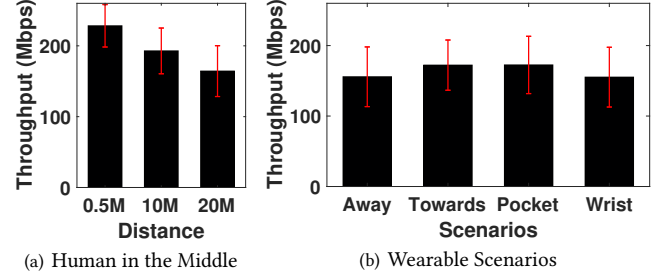

(a) Human in the Middle

(b) Wearable Scenarios

Figure 24: Gateway-to-WiFi Throughput in Mobile Scenarios: In human in the middle scenario, the Gateway-to-WiFi link's throughput can be up to 245.07 Mbps. In different wearable scenarios, our approach maintains similar throughput. This demonstrates that our design can support different types wearable applications.

Figure 23(b) shows four wearable scenarios: i) person walks away from the Chiron gateway with ZigBee sender in pocket; ii) person walks towards from the Chiron gateway with ZigBee sender in pocket; iii) person walks around the meeting room with ZigBee sender in pocket; and iv) person walks around the meeting room with ZigBee attached to the wrist. We can observe the fluctuation across the four wearable scenarios. However, overall, the performance is stable. The lowest throughput still can achieve 188.07 Kbps when the person walks around the meeting room with ZigBee sender in pocket.

Gateway-to-WiFi: Figure 24 shows the throughput of the Gateway-to-WiFi link. In human in the middle (see Figure 24(a)) scenario, the Gateway-to-WiFi link's throughput can be up to 245.07 Mbps. Even when the distance increases to 20 meters, its throughput is still more than 165 Mbps. This indicates that our design is reliable over a long distance. In different wearable scenarios (see Figure 24(b)), our approach maintains similar throughput. This demonstrates that our design can support different types wearable applications.

7 RELATED WORKS

To improve the performance of wireless communication, researchers have proposed various interference mitigate techniques [7, 10, 22, 24, 25, 27, 29] and collision avoidance solutions [19, 20, 26, 28, 29]. To further improve the spectrum utilization, different methods [6, 8, 14, 16, 17, 21, 23, 30, 31, 34, 38] have been proposed. Instead of improving spectrum utilization within the same protocol (i.e., WiFi or ZigBee), our work takes a new approach by exploring the possibility of increasing the spectrum utilization when heterogeneous radios with different protocols are communicating concurrently. Specifically, our approach enables the bi-directional concurrent communication of WiFi and ZigBee.

Several cross-technology communication systems [4, 5, 12, 13, 15, 32, 33, 36, 39, 40] have been introduced, to utilize the coexistent features of different wireless technologies within the same frequency band.

Esense [4] and HoWiES [40] enable WiFi to ZigBee communication by sensing the packet length of WiFi packets. GSense [39] uses special preamble to coordinate heterogeneous devices. FreeBee [15] achieved communication among WiFi, ZigBee and Bluetooth by modulating periodic beacons. EMF [36], C-MORSE [33], DCTC

[13], and WiZig [12] convey cross-technology data at the packet level (i.e., packet length or transmission power). This packet level modulation results a low network performance (i.e., the throughput is at tens or hundreds of bps level). B^2W^2 [5] enables BLE to WiFi transmission by using CSI of WiFi system. WEBee [37] and PMC [35] use WiFi signal to emulate ZigBee signal at the physical layer.

Although WEBee can achieve relatively high CTC throughput, its spectrum utilization is extremely low. This is because when WEBee uses WiFi packets to emulate ZigBee packets, the original payload in the WiFi packets are changed and cannot be used to send out the WiFi data. A single WiFi transmission occupies a 20 MHz channel, while ZigBee receivers only obtain information within a 2MHz-wide ZigBee channel. Since WiFi has more advanced modulation schemes, WiFi can use its 20 MHz channel to transmit WiFi packets at hundreds of Mb/s. By using WEBee, WiFi can only emulate ZigBee packets at 126 Kbps. Therefore, WEBee's spectrum utilization is much lower than original WiFi communication. Similarly, BlueBee [32] also has very low spectrum efficiency, because it uses high throughput Bluetooth signal to emulate low throughput ZigBee signal. Moreover, WEBee, PMC, and BlueBee only provide the communication from one direction (i.e., WiFi or Bluetooth to ZigBee).

Different from the above approaches, our approach enables the concurrent communication from both WiFi and ZigBee devices to the gateway and the reverse direction. By combining or separating the WiFi and ZigBee signal at the bit level, Chiron is able to achieve the similar performance as if in sole WiFi to WiFi or ZigBee to ZigBee communications. Our experimental results demonstrate that our approach's spectrum utilization is more than 16 times higher than traditional approaches.

8 DISCUSSION AND FUTURE WORK

In this section, we discuss the potential opportunities of Chiron.

8.1 Chiron under Different WiFi Standards

WiFi standard includes a variety of generations (from IEEE 802.11 to IEEE 802.11ah and so on). Since Chiron solves the spectrum waste problem while WiFi coexists with ZigBee, we only consider the standard works within 2.4GHz band. As long as the WiFi standard uses OFDM based modulation scheme, such as IEEE 802.11 g/n/ac, Chiron is compatible. That is because the OFDM based modulation scheme chops a wide band (i.e., 20MHz) into small pieces (i.e., 312.5 KHz), which yields a slow symbol rate as we discovered in the motivation section. It is possible that Chiron can support the 40MHz WiFi channel defined by IEEE 802.11n. And more interesting, up to 8 ZigBee channels are overlapped with a 40 MHz WiFi channel. This means that by using Chiron technique, the gateway is able to concurrently communicate with one WiFi device and up to 8 ZigBee devices. In this scenario, the spectrum utilization can be further improved. We will investigate it in our future work.

Multiple-input and multiple-output (MIMO) technique is introduced to WiFi system since IEEE 802.11n. Basically, the MIMO technique increases throughput by spacial multiplexing (i.e, using multiple antennas at both the sender and receiver sides to multiply the channel capacity). For a MIMO enabled WiFi system (e.g., with IEEE 802.11n, a WiFi sender with two antennas and a WiFi receiver with two antennas consist a 2×2 MIMO system), it is possible to enable Chiron technique because the Chiron gateway only needs to transmit one spacial stream to ZigBee device.

8.2 Generality of Chiron

Our Chiron technique explores the possibility to combine WiFi and ZigBee signals. Potentially, Chiron technique can be applied to other wireless communications as long as two communication protocols: i) work on the overlapped frequency bands; and ii) have distinct symbol rates. By having these two properties, it is possible that Chiron can utilize the tolerance of wireless communication to combine two signals with different modulation schemes. However, due to the varieties of different modulation schemes, more future works are needed to investigate different combinations.

8.3 Supports for Upper Layers

With the exponentially increasing number of IoT devices, the traditional multi-radio gateway (e.g., a gateway equipped with both WiFi and ZigBee radios) introduces a spectrum utilization bottleneck, which is caused by the competition between WiFi and ZigBee communications (shown in Figure 1 in the introduction section). Our Chiron technique utilizes the unique properties of WiFi's and ZigBee's physical layers to significantly improve the spectrum utilization. Since Chiron technique does not require any hardware modification on ZigBee device, the original functionalities at upper layers should not be affected, but we have not evaluated that. To further evaluate whether Chiron technique affects the original upper layers' design, we plan to investigate the application profiles such as ZigBee Home Automation (HA), ZigBee Light Link (LL), and building automation in the future. We also plan to investigate how to leverage the Chiron technique for further performance improvements in existing upper layer MAC [41–43], routing [9, 18, 44–46], and flooding protocols [11, 47, 48].

9 CONCLUSION

With the exponentially increasing number of IoT devices, there is a pressing need to more efficiently utilize the spectrum in the crowded ISM band, especially at the edge (i.e., gateway) of the IoT network. In this paper, we explore a new direction – concurrent communication for a gateway to (or from) commodity WiFi and ZigBee devices. Our extensive experimental results indicate that Chiron achieves reliable performance under different settings (i.e., LoS, NLoS, mobile, and wearable). Chiron's concurrent WiFi and ZigBee communication can achieve similar throughput as the sole WiFi or ZigBee communication.

The design principle of Chiron is generic and has the potential to be applied to other frequency band that coexists radios with different symbol rates. The design of Chiron fits naturally at the edge of IoT networks to support commodity WiFi and ZigBee devices. By simply changing the gateway, the spectrum utilization can be increased by more than 16 times.

REFERENCES

[1] https://en.wikipedia.org/wiki/IEEE_802.11n-2009.
[2] http://www.memsic.com/userfiles/files/DataSheets/WSN/telosb_datasheet.pdf.
[3] http://www.zigbee.org/zigbee-for-developers/applicationstandards/zigbee-health-care/.
[4] Chebrolu, K., and Dhekne, A. Esense: Communication through energy sensing. In *MobiCom, 2009.*
[5] Chi, Z., Li, Y., Sun, H., Yao, Y., Lu, Z., and Zhu, T. B2w2: N-way parallel communication for iot devices. In *Sensys, 2016.*
[6] Chintalapudi, K., Radunovic, B., Balan, V., Buettener, M., Yerramalli, S., Navda, V., and Ramjee, R. Wifi-nc: Wifi over narrow channels. In *NSDI, 2012.*
[7] Das, S. M., Koutsonikolas, D., Hu, Y. C., and Peroulis, D. Characterizing multi-way interference in wireless mesh networks. In *WiNTECH, 2016.*
[8] Deek, L., Garcia-Villegas, E., Belding, E., Lee, S.-J., and Almeroth, K. The impact of channel bonding on 802.11n network management. In *CoNEXT, 2011.*
[9] Gu, Y., Zhu, T., and He, T. Esc: Energy synchronized communication in sustainable sensor networks. In *2009 17th IEEE International Conference on Network Protocols* (Oct 2009), pp. 52–62.
[10] Gummadi, R., Wetherall, D., Greenstein, B., and Seshan, S. Understanding and mitigating the impact of rf interference on 802.11 networks. In *SIGCOMM, 2007.*
[11] Guo, S., Kim, S. M., Zhu, T., Gu, Y., and He, T. Correlated flooding in low-duty-cycle wireless sensor networks. In *2011 19th IEEE International Conference on Network Protocols* (Oct 2011), pp. 383–392.
[12] Guo, X., Zheng, X., and He, Y. Wizig: Cross-technology energy communication over a noisy channel. In *IEEE INFOCOM 2017 - IEEE Conference on Computer Communications* (May 2017), pp. 1–9.
[13] Jiang, W., Yin, Z., Kim, S. M., and He, T. Transparent cross-technology communication over data traffic. In *IEEE INFOCOM 2017 - IEEE Conference on Computer Communications* (May 2017), pp. 1–9.
[14] Khan, M., Bhartia, A., Qiu, L., and Lin, K. C.-J. Smart retransmission and rate adaptation in wifi. In *ICNP, 2015.*
[15] Kim, S. M., and He, T. Freebee: Cross-technology communication via free side-channel. In *MobiCom 2015.*
[16] Kumar, S., Cifuentes, D., Gollakota, S., and Katabi, D. Bringing cross-layer mimo to today's wireless lans. In *SIGCOMM, 2013.*
[17] Lee, O., Sun, W., Kim, J., Lee, H., Ryu, B., Lee, J., and Choi, S. Chaser: Channel-aware symbol error reduction for high-performance wifi systems in dynamic channel environment. In *INFOCOM, 2015.*
[18] Malvankar, A., Yu, M., and Zhu, T. An availability-based link qos routing for mobile ad hoc networks. In *2006 IEEE Sarnoff Symposium* (March 2006), pp. 1–4.
[19] Merz, R., Widmer, J., Le Boudec, J.-Y., and Radunovic, B. A Joint PHY/MAC Architecture for Low-Radiated Power TH-UWB Wireless Ad Hoc Networks. Tech. rep., 2004.
[20] Nandagopal, T., Kim, T.-E., Gao, X., and Bharghavan, V. Achieving mac layer fairness in wireless packet networks. In *MobiCom, 2010.*
[21] Panchal, J. S., Yates, R. D., and Buddhikot, M. M. Mobile network resource sharing options: Performance comparisons. *IEEE Transactions on Wireless Communications 12*, 9 (September 2013), 4470–4482.
[22] Prasad, N., Arslan, M., and Rangarajan, S. Enhanced interference management in heterogeneous cellular networks. In *ISIT, 2014.*
[23] Premnath, S. N., Wasden, D., Kasera, S. K., Farhang-Boroujeny, B., and Patwari, N. Beyond ofdm: Best-effort dynamic spectrum access using filterbank multicarrier. In *COMSNETS, 2012.*
[24] Sahai, A., Aggarwal, V., Yuksel, M., and Sabharwal, A. Capacity of all nine models of channel output feedback for the two-user interference channel. *IEEE Transactions on Information Theory 59*, 11 (Nov 2013), 6957–6979.
[25] Salimi, S., Jorswieck, E. A., Skoglund, M., and Papadimitratos, P. Key agreement over an interference channel with noiseless feedback: Achievable region distributed allocation. In *CNS, 2015.*
[26] Sen, S., Choudhury, R. R., and Nelakuditi, S. Csma/cn: Carrier sense multiple access with collision notification. *IEEE/ACM Trans. Netw. 20*, 2 (Apr. 2012), 544–556.
[27] Sen, S., Santhapuri, N., Choudhury, R. R., and Nelakuditi, S. Successive interference cancellation: Carving out mac layer opportunities. *IEEE Transactions on Mobile Computing 12*, 2 (Feb 2013), 346–357.
[28] Shi, J., Aryafar, E., Salonidis, T., and Knightly, E. W. Synchronized csma contention: Model, implementation and evaluation. In *INFOCOM, 2009.*
[29] Singh, N., Gunawardena, D., Proutiere, A., Radunovi, B., Balan, H. V., and Key, P. Efficient and fair mac for wireless networks with self-interference cancellation. In *WiOpt, 2011.*
[30] Sun, L., Sen, S., and Koutsonikolas, D. Bringing mobility-awareness to wlans using phy layer information. In *CoNEXT, 2014.*
[31] Tan, K., Shen, H., Zhang, J., and Zhang, Y. Enable flexible spectrum access with spectrum virtualization. In *DySpan, 2012.*
[32] Wenchao Jiang, Roufeng Liu, Zhimeng Yin, Song Min Kim and T. He. Bluebee: a 10,000x faster cross-technology communication. In *SenSys* (2017).

[33] Yin, Z., Jiang, W., Kim, S. M., and He, T. C-morse: Cross-technology communication with transparent morse coding. In *IEEE INFOCOM 2017 - IEEE Conference on Computer Communications* (May 2017), pp. 1–9.
[34] Yun, S., Kim, D., and Qiu, L. Fine-grained spectrum adaptation in wifi networks. In *MobiCom, 2013.*
[35] Z. Chi, Y. Li, Y. Yao, and T. Zhu. PMC: Parallel Multi-protocol Communication to Heterogeneous IoT Radios within a Single WiFi Channel. In *ICNP* (2017).
[36] Z. Chi, Z. Huang, Y. Yao, T. Xie, H. Sun, and T. Zhu. EMF: Embedding Multiple Flows of Information in Existing Traffic for Concurrent Communication among Heterogeneous IoT Devices. In *INFOCOM* (2016).
[37] Z. Li and T. He. Webee: Physical-layer cross-technology communication via emulation. In *MobiCom* (2017).
[38] Zhang, J., Shen, H., Tan, K., Chandra, R., Zhang, Y., and Zhang, Q. Frame retransmissions considered harmful: Improving spectrum efficiency using micro-acks. In *MobiCom, 2012.*
[39] Zhang, X., and Shin, K. G. Gap sense: Lightweight coordination of heterogeneous wireless devices. In *INFOCOM, 2013.*
[40] Zhang, Y., and Li, Q. Howies: A holistic approach to zigbee assisted wifi energy savings in mobile devices. In *INFOCOM, 2013.*
[41] Zhou, C., and Zhu, T. Highly spatial reusable mac for wireless sensor networks. In *IEEE WiCOM* (2007).
[42] Zhou, C., and Zhu, T. A spatial reusable mac protocol for stable wireless sensor networks. In *IEEE WiCOM* (2008).
[43] Zhou, C., and Zhu, T. Thorough analysis of mac protocols in wireless sensor networks. In *IEEE WiCOM* (2008).
[44] Zhu, T., and Towsley, D. E2r: Energy efficient routing for multi-hop green wireless networks. In *2011 IEEE Conference on Computer Communications Workshops (INFOCOM WKSHPS)* (April 2011), pp. 265–270.
[45] Zhu, T., and Yu, M. A dynamic secure qos routing protocol for wireless ad hoc networks. In *2006 IEEE Sarnoff Symposium* (March 2006), pp. 1–4.
[46] Zhu, T., and Yu, M. Nis02-4: A secure quality of service routing protocol for wireless ad hoc networks. In *IEEE Globecom 2006* (Nov 2006), pp. 1–6.
[47] Zhu, T., Zhong, Z., He, T., and Zhang, Z.-L. Exploring link correlation for efficient flooding in wireless sensor networks. In *Proceedings of the 7th USENIX Conference on Networked Systems Design and Implementation* (Berkeley, CA, USA, 2010), NSDI'10, USENIX Association, pp. 4–4.
[48] Zhu, T., Zhong, Z., He, T., and Zhang, Z. L. Achieving efficient flooding by utilizing link correlation in wireless sensor networks. *IEEE/ACM Transactions on Networking 21*, 1 (Feb 2013), 121–134.